Experimental Evaluation of Material Nano Stability for Ultra Precision Applications

Khaleel Abushgair
Al-Balqa Applied University, Amman, Jordan.

Abstract: *This article presents the construction of a new simple test facility for investigation and testing the materials properties deformation behavior namely; elastic, inelastic and plastic of monolithic spring joints under cyclic loadings. Test samples of 7075-T7351, 7075-T6 and 6061-T6 aluminum alloys were prepared under different machining direction (longitudinal and orthogonal). An electromagnet unit was used as pulling force for sample deformation. The range of the testing load was 0.2 to 200 N raised by a programmable factor of 1.1 to 1.4 at a train time of 15 minutes. The sample deformation with and without loading were measured by using two interferometers and two capacitive sensors placed in a various positions of the sample. The overall testing machine incorporates in a temperature stable housing which provides isothermal conditions. The measured parameters include the inelastic and plastic deformations.*
Key word: *spring joints, plastic deformation, cyclic loadings, precision structure*

I. Introduction

Material stability is a vital characteristic for various ultra precision applications, such as inertial, optical and laser applications [1–5]. The stability under short time loadings (impulse, shock, and vibration), and under medium to long time loadings without load relaxation of internal stress or imbalance are considered an important stability requirements [6–8]. The current article focuses on inertial applications, namely in precision weighing scales. The main components of such scales are the steel mono blocks (mechanical elements). These elements undergo cyclic loadings and attaches to an electromagnetic coil to translate the block deformation to the output display unit in the term of weight. After release the block (each cycle) from the load, it should be returned to its original dimensions with a fast response. And the required time to accomplish this process should be very small and called the time constant of the material. These facts are the disadvantages of the used steel mono blocks in this weighing scale, which is under consideration in this study. Accordingly, the weight measurement process requires ultra precision under high weighing frequency and high stability. Therefore, replacement of these elements by an alternative materials validate the above mentioned characteristics shall be important demand for such scales.

Currently, many typical materials are used for high stability applications such as: chromium and nitrogen containing steels (carbon steels), maraging (non carbon) steels, bronze (mostly the beryllium containing alloys) and titanium. These materials are solution treated, quenched and aged to achieve the required strength. On the other hand, steel have a high undesirable magnetic permeability. Some aluminum based alloys offer the following attractive properties: they are inexpensive, easy to fabricate, and have low modulus of elasticity that results in thicker flexures [9–12].

The main objectives of the present work are to investigate experimentally the mechanical properties of different aluminum alloys namely; 7075-T7351, 7075-T6 and 6061-T6 and to select the most appropriate one to replace the steel mono blocks in high frequency scales.

II. Experimental Setup

2.1. Specimen design

Different aluminum alloy specimens (200 lengths, 40 widths and 20 thicknesses) mm were designed and fabricated. To detect ultra-precision deformation of the specimens two thin flexures (mid cross section of 0.1 X 20 mm^2) were formed with two cutting direction i.e. longitudinal (L)and orthogonal (Q) by using milling CNC machine with diamond tools mounted on a ball bearing spindle. The specimen was mounted in the milling machine at a 3-point, stress free, clamping. Early deformation is prevented by free cutting the flexures at the test starts. As a result, residual stresses from the machining process are kept near the surfaces. Stress relieving was accomplished through heat treatment of the samples. The specimen geometry is shown in figure 1 while figure 2 shows the designation applies to longitudinal and orthogonal cuttings. Longitudinal and orthogonal cuttings means that the cutting direction in spring is tangential at the joint spring radius and radial direction to the fiber diameter spring, respectively.
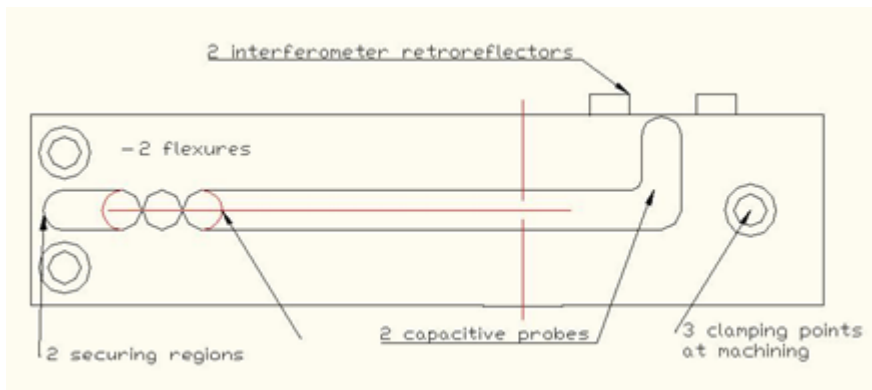
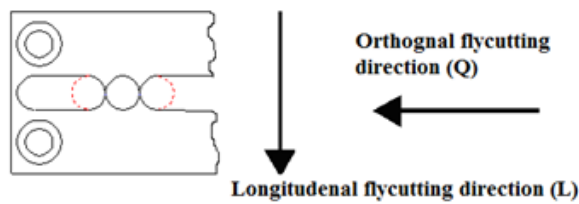**Figure 1.** Specimen geometry

Figure 2. specimen flycuting directions

2.2. Deformation measurement

In this study, ultra-precision measurement of the specimen deformation is considered important demand. For this reason two capacitive sensors and two interferometers were used to measure such deformation. The capacitive sensors are placed the groove of the opposite side of the specimen and is fixed by glue . And the interferometers are placed on the upper surface. In order to obtain magnetic attachment with retro-reflectors, small steel foils were used. In addition, the applying force hook was installed and the interferometer initialized by adjustment of the retro, which can be freely moved on the surface, held in place only magnetically. The deformation was measured at sensors location and has scaled to flexure deformation by the geometry.

2.3 Test machine

The test machine is designed to allow short (1 second) to long (hours) time of loading. The machine composed of four elephant feet, aluminum frame, i.e. clamping frame with quadratic opening to attach the specimen, two cylindrical bearings to gathering the interferometers, and a force transmission wire. The upper plate holds the voice-coil with clamping and the adjustment devices. The coupling of the voice-coil to magnet is augmented by Ferro fluid in the air gap between. Moreover, special care is given to prevent thermal deformations coupling of the voice-coil and magnetic assembly into that of the specimen during measurement. Other parts include a force transducer and electronic devices (not shown in the figure). The schematic test machine is shown in Fig.3.
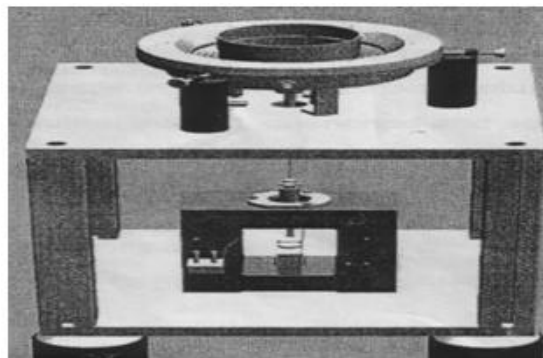

Figure 3. The schematic test machine sketch

III. Experimental procedures

The mechanical properties of the 7075-T7351, 7075-T6 and 6061-T6 aluminum alloys (AA) with different cutting directions were studied herein. For ultra precision measurements, the experimental machine incorporates in a temperature stable housing. Moreover, the temperature of the stable housing was adjusted and controlled for obtaining the same value as the surrounding temperature, with an error of 1 K for all tests. Also the outside vibration of 100 nm was suppressed by isolators to 10 nm and by digital data filtering to below 1 nm. Moreover, Data are gathered during nighttime to minimize temperature, seismic and electric disturbances. To initiate the experiment, the specimen placed in the clamping frame, and then started cyclic loading and unloading with 15 minutes waiting time after releasing the load unloading to separate the inelastic recovery deformation after unloading from plastic deformation. In the next cycle the loading force raised by a programmable factor of 1.1 to 1.4. Typically, a test cycle takes few minutes to allow the storing of capacitive and interferometer data for residual temperature compensating. The experimental conditions are as follows: force loading is ranging from 0.2 to 200 N; resolutions of the interferometer, capacitive sensor, and temperature controller are 10 nm, 0.3 nm, and 0.001 K, respectively. The measured parameters are the inelastic and plastic deformations, and the time constant for aluminum alloy specimens.

For all measured deformation the abbreviations CS and IF indicate the output of the capacitive and interferometer sensors, respectively.

IV. Results and discussion

4.1. Loading and Unloading cycle (cyclic loading)

Figure 4 shows the loading-unloading cycle for the 6061-T6 and 7075-T6 AA group (as an example for all testing steps). As can be shown from the figure the loading cycle starts at 67800 seconds and ends at 70050 seconds (i.e. with 2250 s load application time in the downward direction). However, the unloading starts at 69800 seconds and ends at 74900 seconds. Furthermore, equally important to know that the inelastic recovery is allowed a time up to 3000 s to establish the plastic deformation. In addition, it may be noticed that the inelastic deformation is much lower than plastic deformation and the loading characteristics are therefore in the range up to 40 MPa in their ability statement.
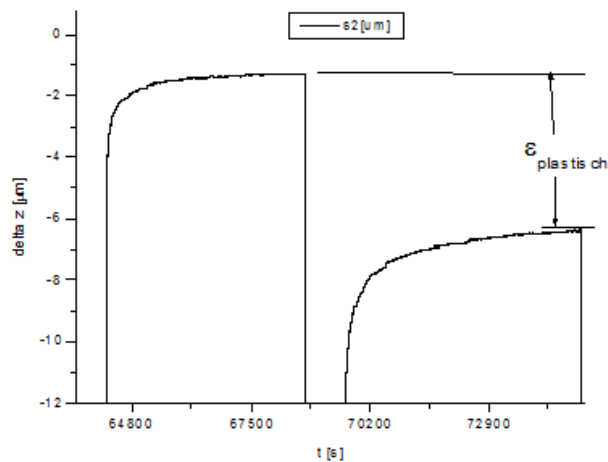

Figure. 4. The loading-unloading cycle

4.2. Inelastic and plastic deformation

Inelastic deformation occurs as a result of the micro-creep in the material that appears due to the movement of the atomic layers in the spring joint during the loading process. After load release, the glides return into their original position. This behavior can vary according to the load on the joints and the pollination period of the last several hours. On the other hand, when increasing the load, the material atoms are farther away from each other without breaking, reaching the yield point, and the plastic deformation occurs. Here the atomic layers are shifted so strongly that if the relief is no longer in their original location back.

The dependence of inelastic deformation on the stress for AA 7075 -T7351 with orthogonal and longitudinal cutting directions are presented in Figs.5a and 5b, respectively. From the figures it may be noticed that the machining direction (weather longitudinal or orthogonal) has a negligible effect on the amount of inelastic deformation due to the fair accuracy of the measuring sensors and the difference in samples properties. The minimum of 1 nm and the maximum of 16 nm deformation were measured under stress values of 10 MPa and 150 MPa, respectively.
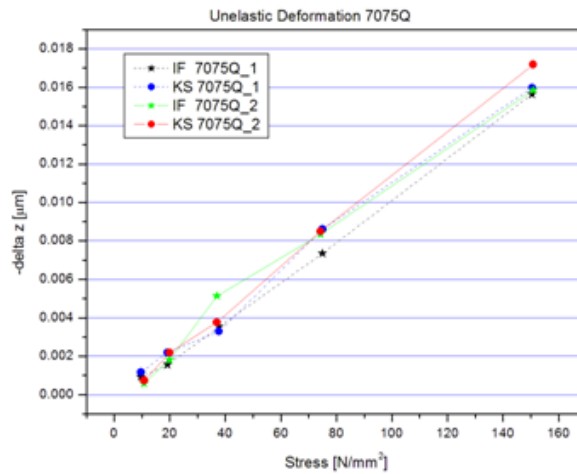
A
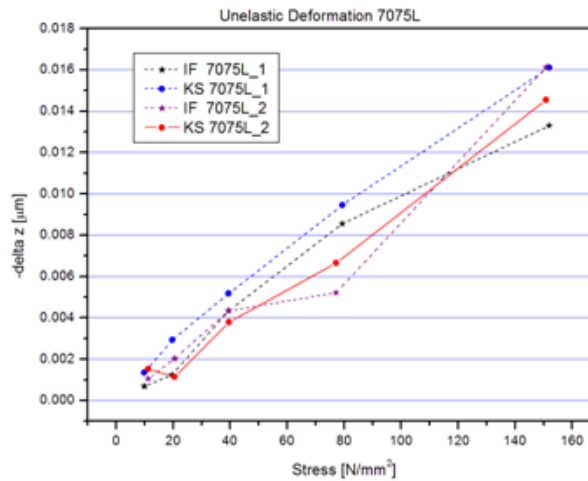
B

Figure 5. Inelastic deformation of 7075 -T7351 aluminum alloy

Plastic deformation for both group of speciments was shown in figures (6a & 6b).specimens of aluminum alloy with orthogonally cutting direction has a plastic deformation of a small bandwidth for each load points. On the other hand, Fig.6b shows aluminum alloy with longitudinal cutting direction and could be marginally better than that of orthogonally cutting, despite the large scattering in the individual measured values. Consequently, the plastic deformation of the 7075- T7351-L AA is less than that of 7075- T7351-Q in the stress interval between 40 and 110 MPa. This can be attributed to the temperature influence and to the electrical drifts of the electronic devices. The plastic deformation is contrary to the tensile stress with two cutting directions (not apparent if only rudimentary). If this interpretation was considered here, only the capacitive sensors should be used up to 40 MPa, because the electrical drift of the interferometer is too large as shown in Fig.6b . It is important here to pay attention to the fact that the plastic deformation of the entire measurement cycle adds the deformations relative to the previous load. The following example explains the plastic deformation between two stress points for both cutting directions. For AA 7075- T7351-L, the deformation mean values were 0.8 nm and 1.1 nm for 80 and 150 MPa stresses, respectively. And the result is plastic deformation of magnitude 0.3 nm. By the same way the deformation of AA 7075- T7351-Q are: 1.1 nm at 80 MPa and 1.5 nm at 150 MPa, and the resulting plastic deformation is 0.4 nm

Comparing with the inelastic deformation, it is important to note that the plastic deformation is lower and therefore the charts are in the range up to 40 MPa in their ability statement.

Plastic Deformation 7075Q

A

Plastisc Deformation 7075L
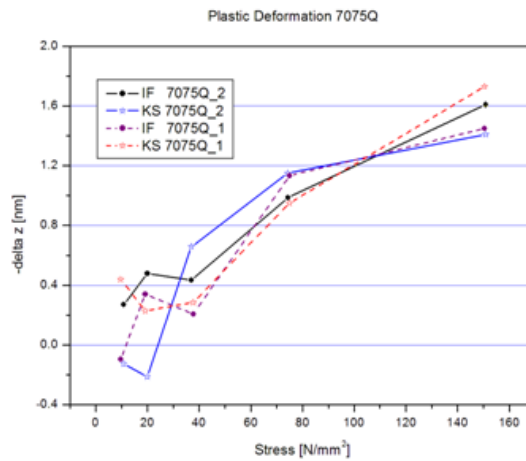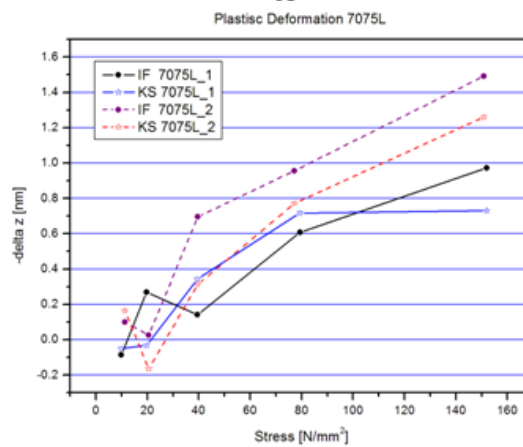
B

Figure 6. Plastic deformation of 7075- T7351 aluminum alloy
A) orthogonelly machined and B) longitudinelly machined

As mentioned above the longitudinal cutting direction mode demonstrate best result for measured deformation than that of orthogonally. hence, only this mode employed on the 6061 T6 and 7075 T6 aluminum alloys .

Figure 7 shows the inelastic deformation of 6061-T6 aluminum alloy against the normal bending stress. The figure shows that, the inelastic deformation at the loading range of 10 to 20 MPa can be set equal to zero, because the identified deformation for trial 1, when capacitive sensor indicates 0.5 nm deformation, can be interpreted as a drift. The same statement applies to the 0.7 nm deformation measured by the interferometer for trial 5. Also from the figure, the maximum average value of the deformation at 150 MPa was 9 nm.

Moreover comparing with the inelastic deformation of 7075-T735 aluminum alloy presented in figure 5, the inelastic deformation of 6061-T6 is slightly lower. For example at stress value equal to 140 N/mm² the inelastic deformation as measured by the capacitive sensor is equal to 10 nm, and 21 nm for the 6061-T6 and 7075-T735 respectively

Figure 9 shows the inelastic deformation of 7075-T6 AA as a function of the normal bending stress. As figure shows at low loads up to 40 MPa, the difference between the deformations measured by CS and IF sensors are small. conversely, when the stress level increases the difference becomes higher. It turns out that one sample in the range of 7075-T7351 (dotted line) is a further trial is worse in all tested tensile stresses. The deviation of the two measurement methods for both samples is within the tolerance range. This shows again that the main influence on the measurement of samples is finished. The difference in thermal treatment has apparently no influence on the inelastic deformation
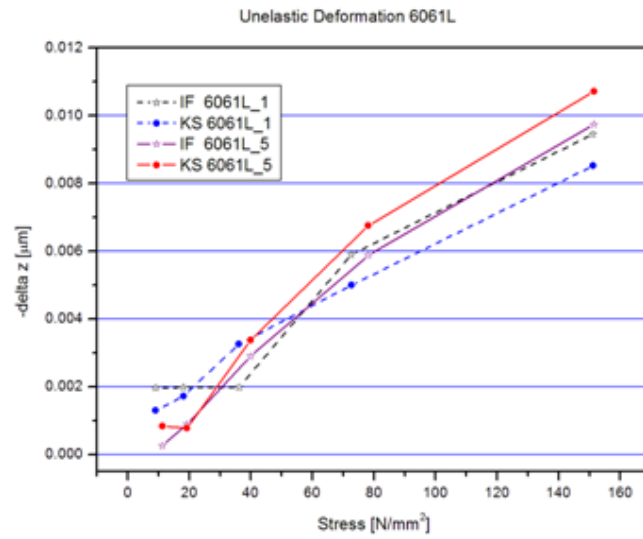
Unelastic Deformation 6061L

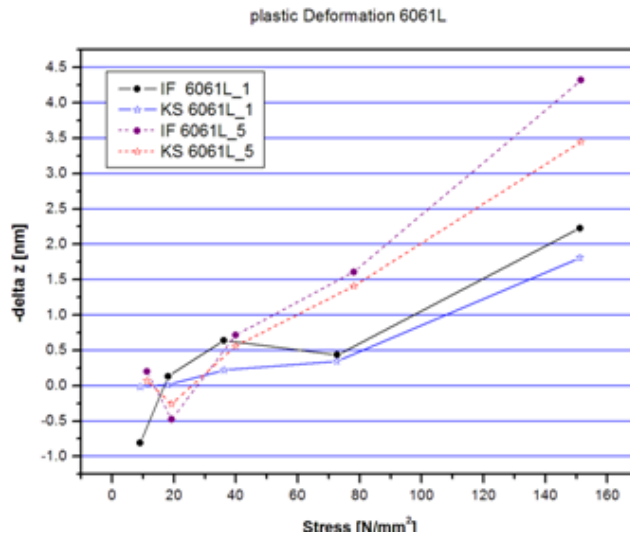**Figure7.** inelastic deformation for 6061- T6 aluminum alloy

plastic Deformation 6061L

Figure 8. Plastic deformation for 6061-T6 aluminum alloy

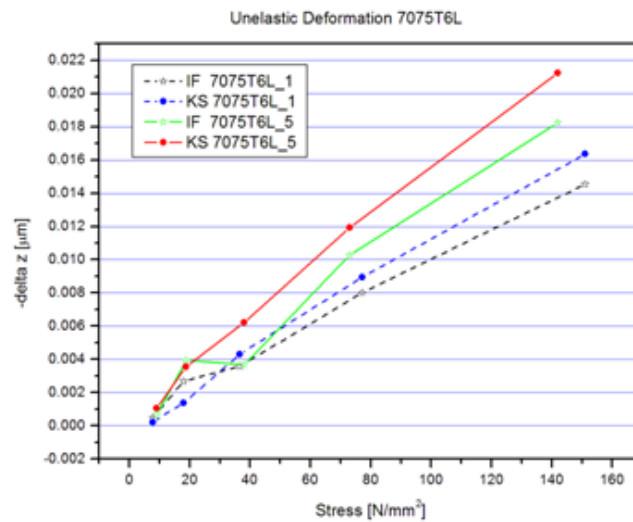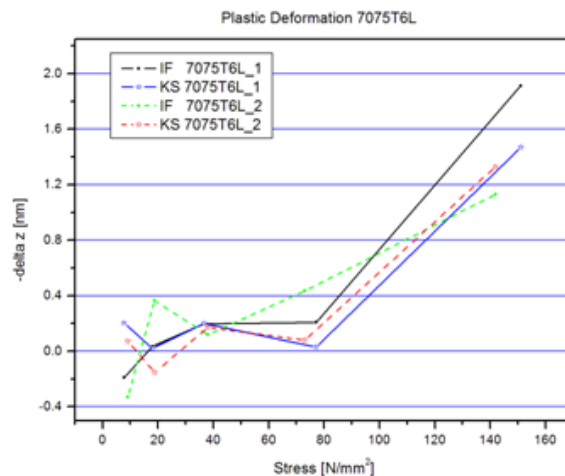**Unelastic Deformation 7075T6L**

Figure 9. inelastic deformation for 7075 -T6 aluminum alloy

Figure 10. Plastic deformation for 7075- T6 aluminum alloy

Plastic deformation for 7075-T6 specimen is presented in figure 10.from the figure it was noted that for astress value up to 80 Mpa the measured plastic deformation is less than 0.4 nm. Then a sudden increase in plastic deformation was recorded between the last two points of thecurve i.e. 80 and 150 Mpa the corresponding increase in the avearge deformation of the specimen is equal to(1,4-0.2)nm

The material 7075T6 compared to an even higher strength, due to the artificial aging and stretching.

V.   Conclusion

This work includes the construction of a new simple test facility for the investigation and testing of materials properties of monolithic spring joints for precision structures. In the test an electromagnet was employed to generate the pulling force necessary for the deformation of the special geometry sample. The deformation and elastic recovery of the samples after pulling force were recorded with the help of an interferometer, and capacitive sensor, for different aluminum alloys(7075-T7351, 7075-T6), with different machining direction (longitudinal and orthogonal).

The results of this work include the inelastic and plastic deformation of the material, and a variation of the load of 10 MPa up to 160 MPa, then the macroscopic deformation after separation of the samples. The test machine incorporates in a temperature stable housing. Measurement is performed down to a residual strain below 10^{-6}.

- Materials nanometer behavior is different from micrometer behavior
- The 6061 T6 material with tensile strength of 275 MPa shows 60% lower inelastic deformation than 7075 T7351 with 435 MPa and 7075T6 with a tensile strength of 505 N / mm ^{2}. Since a difference of 7075 T7351 and 7075 T6 not be identified, is close to the conclusion that regardless of inelastic deformation of the thermal post-treatment of aluminum is crucial here is the alloy composition.
- For the measurement of plastic deformation of the test materials ,the deformation of 7075 L is only 20% lower than in 7075Q.The 7075 T6 material shows a clear difference from 7075 T7351.The low tensile strength and low stress are the main causes of the strongest plastic deformation field in materials from 6061 T6.
- The inelastic deformation between longitudinal and orthogonal cutting direction articulated no differences to recognize.

Acknowledgments

Refrences

[1].   H. Yonezawa, Y. Hirata, H. Sasai, Positioning table with high accuracy and high speed, Annals of the CIRP 39 (1) (1990) 433–436.
[2].   S. Sakuta, K. Ogawa, K. Ueda, Experimental studies on ultra-precision positioning, International Journal of the Japan Society of Precision Engineering 27 (3) (1993) 235–240.
[3].   J.D. Kim, S.R. Nam, An improvement of positioning accuracy by use of piezoelectric voltage in piezoelectric driven micropositioning system simulation, Mechanism and Machine Theory 30 (6) (1995) 819–827.
[4].   P. Ge, M. Jouaneh, Tracking control of a piezoceramic actuator, IEEE Transaction on Control Systems Technology 4 (3) (1996) 209–216.

[5]. S.B. Choi, H.K. Kim, S.C. Lim, Y.P. Park, Position tracking control of an optical pick-up device using piezoceramic actuator, Mechatronics 11 (6) (2001) 691–705.

[6]. S.B. Choi, s.s. Han, A magnification device for precision mechanisms featuring piezoactuators and flexure hinges: Design and experimental validation, Mechanism and machine theory, 42 (2007) 1184–1198.

[7]. J.L. Ha, Y.S. Kung, S.C. Hu, R.F. Fung, Optimal design of a micro-positioning Scott–Russell mechanism by Taguchi method, Sensors and Actuators A: Physical 125 (2) (2006) 565–572.

[8]. VAN HUIS M. A., CHEN J. H., ZANDBERGEN H. W., SLUITER M. H. F. Phase stability and structural relations of nanometer-sized, matrix-embedded precipitate phases in Al-Mg-Si alloys in the late stages of evolution. Acts material, Vol. 54, n°11, . 2006, pp. 2945-2955.

[9]. J.R.Davis, Davis & Associates Aluminium and Aluminium Alloys, ASM Specialty Handbook, 4.Aufl.Ohio, USA, Mai1998

[10]. Craig, W., div.Metals Handbook Ninth Edition, Volume 4, Heat Treating ASM Handbook, 9.Aufl., Ohio, USA, 1998

[11]. ASM Handbook Committee Metals Handbook Ninth Edition, Volume 2, Properties and Selection : Nonferrous and Pure Metals ASM Handbook, 9.Aufl., Ohio, USA, 1998

[12]. Martin L. Culpepper, Gordon Anderson, Design of a low-cost nano-manipulator which utilizes a monolithic, spatial compliant mechanism, Precision Engineering Volume 28, Issue 4, October 2004, Pages 469–482